Available online at www.sciencedirect.com
SCIENCE DIRECT®
Physics Letters A 338 (2005) 247–252
PHYSICS LETTERS A
www.elsevier.com/locate/pla

Global dynamics of dust grains in magnetic planets

Manuel Iñarrea [a,*], Víctor Lanchares [b], Jesús F. Palacián [c], Ana I. Pascual [b], J. Pablo Salas [a], Patricia Yanguas [c]

[a] *Universidad de La Rioja, Área de Física Aplicada, 26006 Logroño, Spain*
[b] *Universidad de La Rioja, Departamento de Matemáticas y Computación, 26004 Logroño, Spain*
[c] *Universidad Pública de Navarra, Departamento de Matemática e Informática, 31006 Pamplona, Spain*

Received 16 November 2004; received in revised form 18 February 2005; accepted 25 February 2005

Available online 8 March 2005

Communicated by A.P. Fordy

Abstract

We study the dynamics of a charged particle orbiting a rotating magnetic planet. The system is modelled by the Hamiltonian of the two-body problem perturbed by an axially-symmetric potential. The perturbation consists in a magnetic dipole field and a corotational electric field. After an averaging process we arrive at a one degree of freedom Hamiltonian system for which we obtain its relative equilibria and bifurcations. It is shown that the system exhibits a complex and rich dynamics. In particular, dramatic changes in the phase flow take place in the vicinity of a circular equatorial orbit, that in the case of Saturn is located inside the E-ring.

PACS: 96.30.Wr; 45.50.Jf; 96.35.Kx

Keywords: Planetary magnetospheres; Størmer problem; Equilibria; Stability and bifurcations; Periodic orbits and invariant tori

1. Introduction

The observations provided by the spacecrafts Voyager, Ulysses and Galileo revealed the presence of innumerable dust grains orbiting around the gaseous planets Jupiter, Saturn, Neptune and Uranus. This dust is scattered not only among the macroscopic bodies of the solid rings but also forms light circumplanetary structures [1]. Besides, the Cassini mission to Saturn has devices for detecting cosmic dust. The analysis of the data obtained from them will give new insights about the charge and size of the dust grains around this giant planet. Other projects such as the Bepi–Colombo mission to explore Mercury's magnetosphere, expected to be launched by ESA in 2008 [2], make crucial the understanding of the motion of charged particles around magnetic planets.

* Corresponding author.
E-mail address: manuel.inarrea@dq.unirioja.es (M. Iñarrea).

0375-9601/$ – see front matter
doi:10.1016/j.physleta.2005.02.038

One of the first attempts towards the study of charged dust was the theoretical approach initiated by Størmer (see [3]) about the motion of a charged particle subject to a dipolar magnetic field. Størmer's analysis provided the framework that led to the understanding of the radiation belts around the Earth and other magnetised planets [4]. These radiation belts are composed by ions and electrons whose motion is well described by using models which take into account only electromagnetic forces. However, dust grains composing faint rings like Saturn's E-ring are much heavier than ions and electrons of radiation belts. It implies that their dynamics cannot be generally well described using solely electromagnetic forces. To overcome this problem, we consider a more realistic physical model that includes the Keplerian gravity, a rotating magnetic dipole of strength μ aligned along the planet's rotating axis and a corotational electric field: the generalised Størmer (GS) model [5,6].

Howard and co-workers [6–8] explore the effective potential governing the dynamics of the GS problem. Besides, the significant question of the global dynamics has been partially treated in [9,10]. In this Letter we focus on the changes in the phase flow that take place in the vicinity of a circular equatorial orbit. These features must be highlighted because they are related to the fine structure of diffuse planetary rings like Saturn's E-ring. The origin and structure of this kind of rings remains as an open question in the literature.

2. Dynamical model and its average

For a dust grain of mass m and charge q orbiting around a magnetic planet of mass M and radius R which rotates with angular velocity ω, the GS Hamiltonian in Gaussian units and cylindrical coordinates $(\rho, z, \phi, P_\rho, P_z, P_\phi)$ is:

$$\mathcal{H} = \frac{1}{2m}\left(P_\rho^2 + P_z^2 + \frac{P_\phi^2}{\rho^2}\right) - \frac{Mm}{r} - \omega_c R^3 \frac{P_\phi}{r^3} + \frac{m\omega_c^2 R^6}{2}\frac{\rho^2}{r^6} + m\omega\omega_c R^3 \frac{\rho^2}{r^3}, \tag{1}$$

where $r = \sqrt{\rho^2 + z^2}$, $B_o = \mu/R^3$ is the magnetic field strength at the equator of the planet and $\omega_c = (qB_o)/(mc)$ is the cyclotron frequency, being c the speed of the light in the vacuum. Due the axial symmetry of the system, the z-component of the angular momentum, P_ϕ, is conserved and the system defined by (1) has two degrees of freedom. To analyse its dynamics it is convenient to use dimensionless coordinates as a function of the planet radius R and the Keplerian frequency $\omega_K = (M/R^3)^{1/2}$. After these considerations, we get:

$$\mathcal{H} = \frac{P_\rho^2}{2} + \frac{P_z^2}{2} + \frac{P_\phi^2}{2\rho^2} - \frac{1}{r} - \delta\frac{P_\phi}{r^3} + \delta\beta\frac{\rho^2}{r^3} + \delta^2\frac{\rho^2}{2r^6}, \tag{2}$$

where the parameters $\delta = \omega_c/\omega_K$ and $\beta = \omega/\omega_K$ indicate, respectively, the ratio between the magnetic and the Keplerian interactions (e.g., the charge–mass ratio q/m of the particle) and the ratio between the electrostatic and Keplerian interactions. For a given planet, B_o, ω and ω_K are constant and thence the problem depends on the three parameters P_ϕ, $\mathcal{H}$ (the energy), and δ. For a more detailed description of the model we address to [9] and references therein. If the gravity dominates ($|\delta| \ll 1$), Hamiltonian (2) can be understood as a sum of a pure Keplerian part, and a perturbation describing the electromagnetic forces. For instance, this situation takes place for micron-size dust grains forming Saturn's E-ring [5,11].

Our approach is purely analytical. The basic idea is to transform Hamiltonian (2) into an integrable approximation via averaging. Delaunay variables (ℓ, g, h, L, G, H) are a suitable set to achieve the normalisation in a Keplerian-type system. Variable L is the Delaunay action related to the unperturbed Keplerian energy $\mathcal{H}_0 = -1/(2L^2)$, G is the modulus of the angular momentum and $H = P_\phi$. The corresponding angles ℓ, g and h represent, respectively, the mean anomaly, the argument of the pericentre and the ascendant node of the orbit in the instantaneous orbital plane.

The averaging method is the so-called Delaunay normalisation, i.e., a near-identity canonical change of variables whose goal is to transform a perturbation of the two-body Hamiltonian into another one which has the action L as a new integral [12]. Up to first order, the new Hamiltonian is given by $\mathcal{K} = \mathcal{K}_0 + \mathcal{K}_1$ with

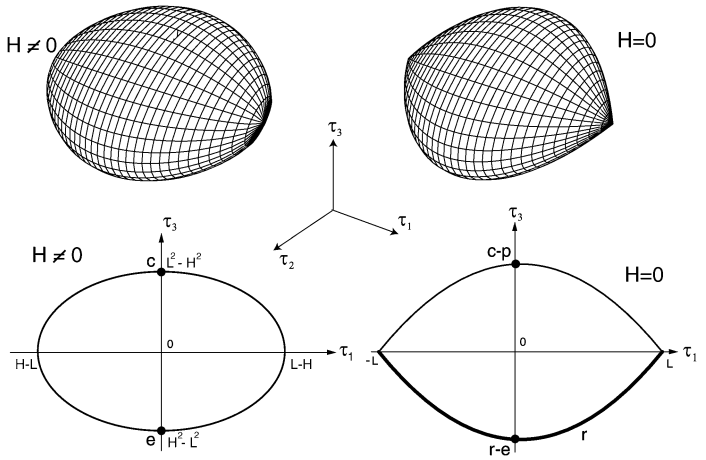

Fig. 1. Top: phase space $\mathcal{T}_{L,H}$ (left) and $\mathcal{T}_{L,0}$ (right). Bottom: projections of $\mathcal{T}_{L,H}$, $0 \leqslant |H| < L$, onto the plane $\tau_2 = 0$; on the left, **c** stands for circular orbits while **e** represents equatorial orbits; on the right, **r** is the arc corresponding to rectilinear trajectories, while **r**-**e** denotes rectilinear orbits in the equatorial plane and **c**-**p** are circular-polar trajectories.

$\mathcal{K}_0 = -1/(2L^2)$ and

$$\begin{aligned}\mathcal{K}_1 = {} & \frac{\delta}{16L^5(L+G)G^7} \\ & \times \big[2(L+G)\big(4\beta L^3G^7 + 4\beta L^3G^5H^2 - \delta G^4 \\ & - 8L^2G^4H - \delta G^2H^2 + 3\delta L^2G^2 + 3\delta L^2H^2\big) \\ & + (L-G)\big(G^2 - H^2\big) \\ & \times \big(8\beta L^3G^5 + \delta G^2 + 2\delta LG + \delta L^2\big)\cos(2g)\big].\end{aligned}$$

For a fixed $L > 0$, the phase space related to Keplerian-like Hamiltonians independent of ℓ is the product of the two spheres $S^2_L \times S^2_L$ [13]. However, if the Hamiltonian enjoys an axial symmetry, it may be further reduced to a compact two-dimensional space [14] $\mathcal{T}_{L,H} = \{(\tau_1, \tau_2, \tau_3) \in \mathbf{R}^3\}$, where

$$\begin{aligned}&\tau_2^2 + \tau_3^2 = \big[(L+\tau_1)^2 - H^2\big]\big[(L-\tau_1)^2 - H^2\big], \\ &\quad \tau_1 \in [H-L, L-H]. \end{aligned} \tag{3}$$

The relationship between (g, G) and (τ_1, τ_2, τ_3) is:

$$G^2 = \frac{1}{2}\big(L^2 + H^2 - \tau_1^2 + \tau_3\big),$$

$$\cos g = \frac{-\tau_2}{\sqrt{(L^2-H^2)^2 - (\tau_1^2 - \tau_3)^2}},$$

$$\sin g = \tau_1\sqrt{\frac{2(L^2 + H^2 - \tau_1^2 + \tau_3)}{(L^2-H^2)^2 - (\tau_1^2 - \tau_3)^2}}.$$

A representation of the space $\mathcal{T}_{L,H}$ is given in Fig. 1.

Hamiltonian $\mathcal{K}$ is now written in terms of the τ_i's, after dropping constant terms, as:

$$\begin{aligned}\mathcal{K} = {} & \frac{\delta}{4L^5\tau_4^7[4L\tau_4 + \sqrt{2}(2L^2 + \tau_4^2)]} \\ & \times \big\{\delta\big(2L^2 + 2\sqrt{2}L\tau_4 + \tau_4^2\big) \\ & \times \big[\tau_4^2\big(14L^2 - 4\tau_1^2 - 3\tau_4^2\big) + H^2\big(20L^2 - 2\tau_4^2\big)\big] \\ & + 8L^2\tau_4^4\big[-2H\big(2L^2 + 2\sqrt{2}L\tau_4 + \tau_4^2\big) \\ & + \beta L\tau_4^2\big(2H^2L + \sqrt{2}\big(L^2 + H^2 - \tau_1^2\big)\tau_4 \\ & + L\tau_4^2\big)\big]\big\},\end{aligned}$$

where we write $\tau_4 = \sqrt{L^2 + H^2 - \tau_1^2 + \tau_3}$. The phase flow for $\mathcal{K}$ is mainly managed by its equilibria and their stability.

3. Relative equilibria and bifurcations

Equilibrium points are obtained as the local extrema of $\mathcal{K}$ on $\mathcal{T}_{L,H}$. A detailed analysis about the existence conditions and linear stability is given in [9], where those terms in δ^2 are neglected. From this analysis a number of parametric bifurcation lines are determined, both for prograde ($H > 0$) and retrograde ($H < 0$) motions. On the one hand, for $H > 0$ we get

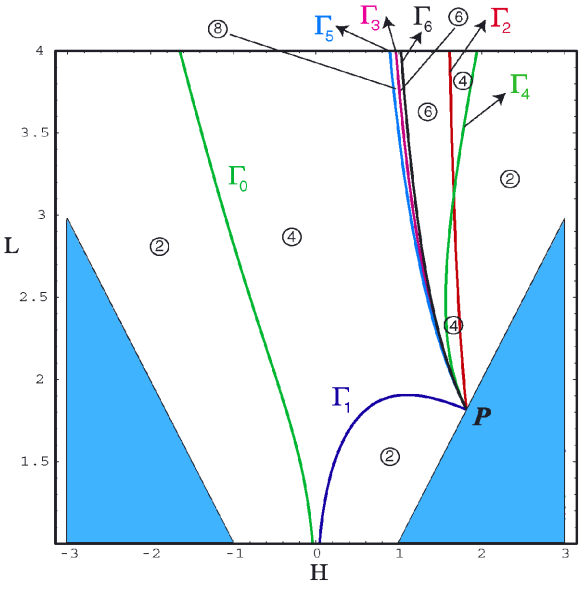

Fig. 2. Plane of parameters (H, L) for $\delta = 0.01$ and $\beta = 0.4$. The number of equilibria in each region is encircled.

the lines

$$\begin{aligned}
&\Gamma_1 \equiv 3\beta L^2 H^2 + \beta L^4 - 12H = 0,\\
&\Gamma_2 \equiv 2\beta L H^3 - 3(L+H) = 0,\\
&\Gamma_3 \equiv 2\beta L^2 H^2 - 3(L+H) = 0,\\
&\Gamma_4 \equiv \beta L^2\left(L^2 - 5H^2\right) + 12H = 0,\\
&\Gamma_5 \equiv -3H + 8\beta L^2 H^2 - 16\beta L^4\\
&\qquad - 6\beta^2 L^4 H^3 + \beta^4 L^8 H^5 = 0,\\
&\Gamma_6 \equiv \beta L^2 H^2 (L+H) - 2\left(L^2 + LH + H^2\right) = 0. \quad (4)
\end{aligned}$$

On the other hand, for $H < 0$ we get

$$\Gamma_0 \equiv 5\beta L^2 H^2 - \beta L^4 - 12H = 0. \quad (5)$$

It is worth to note that if the terms in δ^2 are taken into account, new bifurcation lines appear; moreover, the lines addressed before are slightly modified. Nevertheless, the new lines, that involve new equilibrium points, are not of physical interest as they are in correspondence with collision type orbits. Indeed, as they are related to Keplerian trajectories, their pericentres are located inside the planet, that is, at a distance smaller than 1. In this way, after fixing a value of L, the most eccentric non-collisional orbit satisfies $L^2\sqrt{1 - H^2/L^2} = 1$. This equation defines a curve

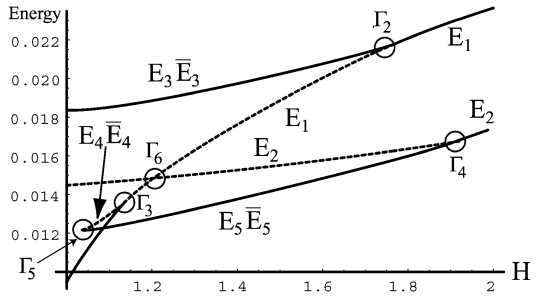

Fig. 3. Evolution of the energy for the equilibrium points when $L = 2.5$ and H varies from 1 to 2. Dashed lines stand for unstable equilibria, whereas solid lines stand for stable points. Circles represent bifurcations.

in the parameter plane (H, L) that separates collision motions from non-collisional ones. As we are interested in a qualitative description of circumplanetary trajectories, it is enough with analysing the model with $\delta^2 = 0$.

Taking into account all the above, it follows that, for a fixed β, the plane (H, L) is divided into different regions where the number of equilibria changes. These regions are determined by the curves (4) and (5) together with the constraint $|H| \leqslant L$ as it is depicted in Fig. 2. There always exist two equilibrium points E_1 and E_2 corresponding to the class of equatorial and circular trajectories, respectively. The rest of equilibria, when they exist, appear as pairs. Points E_3, $\bar{E}_3$ are symmetric with respect to the plane $\tau_2 = 0$, whereas E_4, $\bar{E}_4$ and E_5, $\bar{E}_5$ are symmetric with respect to $\tau_1 = 0$.

4. Discussion

Remark 1. As the flow of the Hamiltonian is defined over a compact space, $\mathcal{T}_{L,H}$, if an equilibrium point is stable it corresponds to a maximum or a minimum, whereas if it is unstable its energy takes an intermediate value. Hence, we are able to determine the stability of the equilibria by studying the evolution of their energies, as the parameters (H, L) take values in the different regions of Fig. 2. For instance, in Fig. 3 it is depicted the energy of the equilibrium points for $L = 2.5$ as H varies from 1 to 2.

Remark 2. All the lines Γ_k correspond to parametric bifurcations of pitchfork type except for Γ_5 that

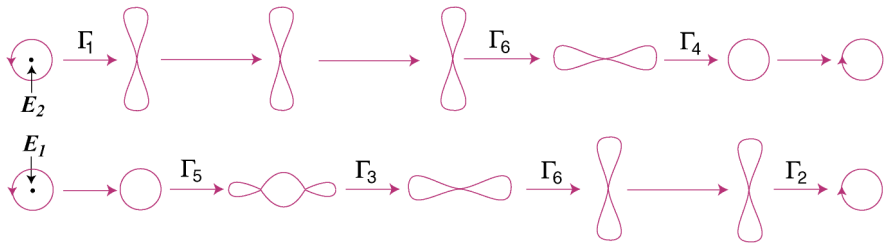

Fig. 4. Sketch of the sequence of bifurcations of the class of circular (E_2) and equatorial (E_1) orbits as the bifurcation lines are crossed. Direction of the flow is viewed from the positive axis τ_3.

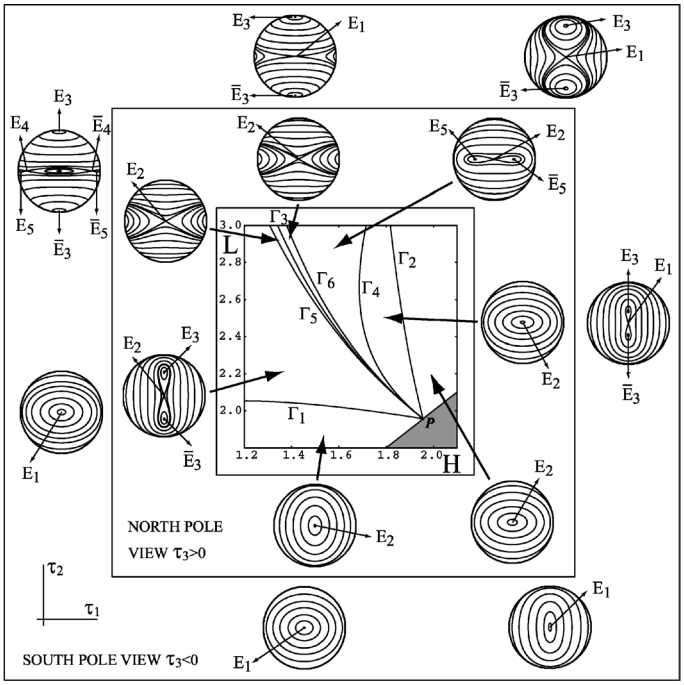

Fig. 5. Different types of flow in the phase space $\mathcal{T}_{L,H}$ over the parametric plane (H, L) for $\delta = 0.01$ and $\beta = 0.4$, showing north- and south-pole views. We present the phase space like a sphere to get a better visualisation of the phase flow evolution.

corresponds to a saddle-centre bifurcation and Γ_6 to a saddle connection. This conclusion follows from the number of equilibrium points involved in the bifurcations together with the index theorem and a theorem on the multiplicity of a root for a vanishing discriminant. A sketch of the sequence of bifurcations is depicted in Fig. 4.

Remark 3. An outstanding feature is the presence of a saddle-connection bifurcation when both E_1 and E_2 are unstable and the energy of their orbits is the same. This is a global bifurcation and not a local one. As a consequence, the flow direction around E_1 and E_2 reverse when crossing Γ_6 (see Fig. 4). The physical meaning is that the advance of the pericentre of the osculating ellipse is clockwise or counter-clockwise.

Remark 4. All the curves are coincident at the point

$$P \equiv \left(\sqrt[3]{3/\beta}, \sqrt[3]{3/\beta}\right)$$

on the line $L = H$. This point corresponds to an equatorial circular orbit around which the dynamics is extremely complex. The orbit corresponding with the point P is a periodic orbit of the original system and it

remains Keplerian in spite of the perturbation. Even more, the characteristic frequencies associated with this orbit are in resonance 1:1. This can be inferred from the Hessian matrix associated with Hamiltonian (2) evaluated at point P.

Remark 5. Associated with each relative equilibria there is a family of (approximate) two-dimensional invariant tori in the original Hamiltonian (1) parameterised by the angles ℓ and h. These tori are functions of the actions L and H and are filled up with quasiperiodic trajectories. Using the implicit function theorem [15], we may guarantee the existence of families of invariant tori close to the approximated ones we have computed. Moreover, the bifurcation lines and the stability of the equilibria are translated into the bifurcations and the stability character of the invariant tori. Besides, it is possible to obtain some periodic orbits out of the quasiperiodic orbits using the discrete symmetries of the Hamiltonian (see [9]).

A picture of the phase flow in each region around the point P is depicted in Fig. 5. It is important to highlight that a small change in the value of the parameters near the point P yields dramatic changes in the dynamics. In fact, as it can be seen in Fig. 5, the number of equilibrium points may vary from 2 to 8 through an appropriate sequence of bifurcations. Consequently, a rich scenario of periodic and quasiperiodic orbits is expected near the equatorial circular orbit associated to P specially for low inclinations and eccentricities.

5. Conclusions

In spite of its simplicity, the generalised Størmer model exhibits a very rich dynamics specially around the point P of the parametric plane where all the bifurcation lines meet. Moreover at this point a 1:1 resonance occurs and branches of relative periodic orbits emanate from it.

In the case of Saturn ($\beta \approx 0.4$), the orbit associated to P is located at about $3.8R$, inside the E-ring, but very close to its beginning. The presence of the Saturn's moon Enceladus in the vicinity of the circular orbit defined by point P can help to explain the dynamics and structure of the dusty E-ring. In particular, the 1:1 resonance could be the responsible of the ring's narrowing about $3.8R$. However, the inclusion in the model of the oblateness of Saturn and the radiation pressure [5] should be taken into account in order to refine our conclusions.

Acknowledgements

Work supported by projects #BFM2002-03157 of Ministerio de Ciencia y Tecnología (Spain) and #ACPI2002/04 of Gobierno de La Rioja (Spain).

References

[1] A.M. Fridman, N.N. Gor'kavyi, Physics of Planetary Rings: Celestial Mechanics of Continuous Media, Springer-Verlag, Berlin, 1999.
[2] R. Grard, A. Balogh (Eds.), Returns to Mercury: Science and Mission Objectives, Planet. Space Sci. 49 (2001) 1395 (special issue).
[3] C. Størmer, Arch. Sci. Phys. Nat. 24 (1907) 5;
C. Størmer, Arch. Sci. Phys. Nat. 24 (1907) 113;
C. Størmer, Arch. Sci. Phys. Nat. 24 (1907) 221;
C. Størmer, The Polar Aurora, Clarendon Press, Oxford, 1955.
[4] M. Braun, SIAM Rev. 23 (1981) 61.
[5] D.P. Hamilton, Icarus 101 (1993) 244;
D.P. Hamilton, Icarus 103 (1993) 161, Erratum.
[6] J.E. Howard, M. Horányi, G.E. Stewart, Phys. Rev. Lett. 83 (1999) 3993.
[7] H.R. Dullin, M. Horányi, J.E. Howard, Physica D 171 (2002) 178.
[8] J.E. Howard, H.R. Dullin, M. Horányi, Phys. Rev. Lett. 84 (2000) 3244.
[9] M. Iñarrea, V. Lanchares, J.F. Palacián, A.I. Pascual, J.P. Salas, P. Yanguas, Physica D 197 (2004) 242.
[10] M. Iñarrea, V. Lanchares, J.F. Palacián, A.I. Pascual, J.P. Salas, P. Yanguas, Monograf. Acad. Ci. Exact. Fís.-Quím. Nat. Zaragoza 25 (2004) 159.
[11] T.W. Hartquist, O. Havnes, G.E. Morfil, Astron. Geophys. 44 (2003) 5.26.
[12] A. Deprit, Celestial Mech. 26 (1982) 9.
[13] J. Moser, Commun. Pure Appl. Math. 23 (1970) 609.
[14] R.H. Cushman, Celestial Mech. 31 (1983) 401.
[15] J. Palacián, Chaos 13 (2003) 1188.